XV-15 Tiltrotor Low Noise Approach Operations

David A. Conner
Aeroflightdynamics Directorate (AVRDEC), U.S. Army Aviation and Missile Command
Langley Research Center
Hampton, VA 23681-2199

Michael A. Marcolini
Aero Performing Center Program Management Office
NASA Langley Research Center
Hampton, VA 23681-2199

William A. Decker
Flight Control and Cockpit Integration Branch, Army/NASA Rotorcraft Division
NASA Ames Research Center
Moffett Field, CA 94035-1000

John H. Cline
Vehicle Technology Center, Army Research Laboratory
Langley Research Center
Hampton, VA 23681-2199

Bryan D. Edwards
Colby O. Nicks
Peter D. Klein
Bell Helicopter Textron, Inc.
Fort Worth, TX 76101

Abstract

Acoustic data have been acquired for the XV-15 tiltrotor aircraft performing approach operations for a variety of different approach profile configurations. This flight test program was conducted jointly by NASA, the U.S. Army, and Bell Helicopter Textron, Inc. (BHTI) in June 1997. The XV-15 was flown over a large area microphone array, which was deployed to directly measure the noise footprint produced during actual approach operations. The XV-15 flew realistic approach profiles that culminated in IGE hover over a landing pad. Aircraft tracking and pilot guidance was provided by a Differential Global Positioning System (DGPS) and a flight director system developed at BHTI. Approach profile designs emphasized noise reduction while maintaining handling qualities sufficient for tiltrotor commercial passenger ride comfort and flight safety under Instrument Flight Rules (IFR) conditions. A discussion of the approach profile design philosophy is provided. Five different approach profiles are discussed in detail -- 3°, 6°, and 9° approaches, and two very different 3° to 9° segmented approaches. The approach profile characteristics are discussed in detail, followed by the noise footprints and handling qualities. Sound exposure levels are also presented on an averaged basis and as a function of the sideline distance for a number of up-range distances from the landing point. A comparison of the noise contour areas is also provided. The results document the variation in tiltrotor noise due to changes in operating condition, and indicate the potential for significant noise reduction using the unique tiltrotor capability of nacelle tilt.

Presented at the American Helicopter Society 55th Annual Forum, Montreal, Quebec, Canada, May 25-27, 1999.

Introduction

Many U.S. airports are rapidly reaching their saturation point with regard to the number of daily aircraft operations permitted. Commuter aircraft, flying fairly short routes with relatively few passengers, make up a significant portion of the total airport operations, thus limiting the total number of passengers that can use that airport each day (Ref. 1). Tiltrotor aircraft, with their unique capability to take off and land vertically while still flying like an airplane during cruise, provide a potential alternate means of transportation that could link major cities, thus alleviating some of the demand on airports. Research on tiltrotor aircraft has been

conducted for many years using such vehicles as the XV-3 and the XV-15, among others. More recently, the Navy has begun procurement of the V-22 Osprey to utilize the capabilities of the tiltrotor for military applications. However, noise generated by the large tiltrotor aircraft is a potential barrier issue for civil market penetration. Reference 2 provides a review of tiltrotor aeroacoustics, describing the primary noise sources, as well as reviewing the state-of-the-art at that time, both experimentally and analytically.

The XV-15 has been the predominant tiltrotor research aircraft for approximately the last 20 years. As a joint NASA/Army/Bell venture, two XV-15 aircraft were built, and much acoustic testing has been accomplished using these vehicles. Lee and Mosher (Ref. 3) showed significant variation (10-15 dB) in noise level as a function of nacelle tilt angle in a test of an XV-15 in the NASA Ames 40x80 Foot Wind Tunnel. However, detailed directivity changes could not be measured because only four microphones were used. Both Maisel and Harris (Ref. 4) and Conner and Wellman (Ref. 5) conducted XV-15 flight tests that successfully mapped the aircraft noise directivity during hover for two different rotor blade sets. Brieger, Maisel, and Gerdes (Ref. 6) conducted XV-15 flight tests, acquiring acoustic data during level flight, ascent, and descent operating conditions. The results of Reference 6 show significant variation in noise generation with nacelle tilt, but since acoustic data were only acquired at two sideline angles to each side of the aircraft; directivity information was again limited. Edwards (Ref. 7), in another XV-15 acoustics flight test, acquired data using a large array for the purposes of obtaining noise footprint data, but only for a very limited test matrix. In a joint NASA/Army/Bell Helicopter Textron test of a model tiltrotor in the 14- by 22-Foot Subsonic Tunnel at the NASA Langley Research Center, Marcolini et al. (Ref. 8) again show significant variations in both noise level and directivity as a function of rotor operating condition. More recently, Conner et al. (Ref. 9) conducted extensive XV-15 flight tests in a two-phase test program. Phase 1 used a linear microphone array to successfully map the noise directivity for many different ascent, descent, and level flight operating conditions. During phase 2 of this test, ground noise footprints were measured using a large area microphone array, but only for a limited number of approach and take-off conditions.

There are two obvious ways to reduce the noise produced by a tiltrotor aircraft. One approach is to design a quieter rotor. However, this is an approach that requires a significant lead time and involves complex aeroacoustic and structural design tradeoffs. A second approach is to make use of the nacelle tilt capability of a tiltrotor, which allows the aircraft to fly a specified flight path at a number of different rotor operating conditions. In the present paper, results are presented from a 1997 flight test of the XV-15 that addresses this second approach. The test was conducted under the sponsorship of the Short Haul Civil Tiltrotor element of the NASA Aviation Systems Capacity Program. Results from acoustic measurements of realistic approaches are presented. These results document the variation in tiltrotor noise due to changes in operating condition, and indicate the potential for significant noise reduction using the unique tiltrotor capability of nacelle tilt. In addition, discussions of the tracking and guidance systems are included, as well as discussions of the approach profile design philosophy.

Experimental Setup

During this test meteorological, tracking, and XV-15 state data were all acquired simultaneously with the acoustic data. GPS satellite time-code was recorded on all data recorders to provide for synchronization of all data sets.

XV-15 Tiltrotor Aircraft

The XV-15 tiltrotor aircraft (Figure 1) was built by Bell Helicopter Textron, Inc. (BHTI), as a proof of concept aircraft and technology demonstrator whose first flight was in May 1977. The XV-15 has two 25-foot diameter rotors mounted on pivoting nacelles that are located on the wing tips. Each nacelle houses a main transmission and a Lycoming T-53 turboshaft engine capable of generating 1800 shaft horsepower. The nacelles are tilted into the vertical position (90° nacelle angle) for vertical takeoffs and landings and rotated to the horizontal (0° nacelle angle) for cruising flight. Each rotor has three highly twisted, square-tip, stainless steel blades which typically operate at 589 RPM during hover and transitional flight modes, and at 517 RPM in cruise, corresponding to 98% and 86% of rotor design speed. The wings have a 6.5° forward sweep to provide clearance for rotor flapping. During this test, the nominal vehicle takeoff gross weight was 13,900 pounds, including about 2000 pounds of fuel. During the period of data acquisition, fuel burn-off resulted in an approximately 10% reduction in the vehicle gross weight. The vehicle was operated by BHTI under contract to NASA. In addition, BHTI furnished research pilots, flight test engineers, ground crew personnel, and other necessary support personnel for operation and maintenance of the aircraft and on-board data acquisition system. A more detailed description of the XV-15 aircraft is available in reference 10.

Figure 1. XV-15 hovering at test site.

The XV-15 featured an impressive suite of on-board instrumentation. Approximately 150 aircraft state parameters were measured and recorded on magnetic tape. Transducers included attitude and rate gyros, strain gauges, temperature sensors, accelerometers, and control position sensors. In addition to the standard on-board instrumentation package, a Differential Global Positioning System (DGPS) and flight director system were installed to provide tracking and pilot guidance.

The XV-15 flight envelope, shown in Figure 2, illustrates the combination of nacelle angle and airspeed necessary to achieve stabilized level flight conditions. It should be noted that a fairly broad range of nacelle angles and airspeeds is possible within this operating envelope. The acoustic effects of avoiding certain portions of this range can guide flight operations of the XV-15 (and presumably other tiltrotor aircraft) in minimizing external noise. The present test was designed to define and quantify these effects during approach conditions.

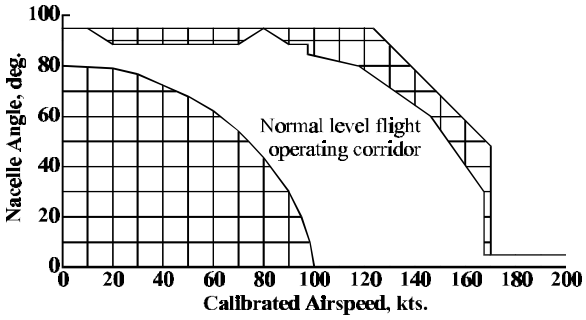

Figure 2. XV-15 flight envelope.

Differential Global Positioning System

A 12-channel, dual frequency Ashtech Model Z-12 GPS receiver was installed on board the XV-15 during this test. This unit provides serial data outputs for corrected position, as well as velocity, correction data status, and satellite information. The receiver also stores the raw data for each position solution, which allows optional post-processing of the position and velocity data. The GPS antenna was located on top of the fuselage, aft of the wing. This location has proven to yield good reception of the satellite signals. Differential corrections were received from a reference ground GPS unit using a VHF radio modem. The antenna for the correction link was located on the belly of the aircraft behind the cockpit.

The GPS reference ground station consisted of a matching GPS receiver and radio modem. A survey-type GPS antenna and the antenna for transmission of the correction information were located on the roof of the BHTI telemetry data van, which was located at the test site. Position and velocity solutions can be calculated at rates up to 5 Hz. Differential corrections were determined and transmitted to the aircraft twice per second at 19,200 baud.

The information from the onboard DGPS receiver was passed from a serial data port to a Bell-designed interface unit. This unit parsed the serial GPS data stream and formatted the values into data words, which were inserted into the aircraft's pulse-code modulated (PCM) data stream. This approach allowed the GPS measurements to be correlated in time with the remainder of the approximately 150 measured aircraft parameters. The PCM data stream, including the GPS parameters, was simultaneously recorded on the aircraft and transmitted to the telemetry data van for real-time monitoring.

Flight Director

The XV-15 was fitted with a Silicon Graphics, Inc. computer that calculated flight director guidance parameters to perform the precision approaches required for this flight test program (Ref. 11). The computer received DGPS information and other aircraft state parameters by means of an ethernet communications link with the interface unit. The flight director computer utilized guidance control laws developed in NASA/Bell simulations specifically for tiltrotor operations (Ref. 12).

The flight director provided guidance commands for the desired aircraft configuration as well as for the desired flight path and velocity profile. Commands were given for the operation of flaps, landing gear, and nacelle conversion angle. The nacelle conversion angle and flaps can be used very effectively to reduce pilot workload and control fuselage attitude while flying very precise approach paths.

The XV-15 copilot's instrument panel was modified with the installation of a color liquid crystal display (LCD). The display, shown in Figure 3, provided essential information for piloting the aircraft, and also provided the information needed for flight director guidance. Conventional command bars were used for flight path guidance, and raw data for horizontal and vertical errors were also provided. Ground speed errors were displayed, and power lever commands were given for airspeed and descent rate control.

Figure 3. Flight director cockpit display.

Meteorological Instrumentation

Two data systems were used to acquire weather information, a tethered weather balloon system and a weather profiler system. The tethered weather balloon system consisted of an electric winch-controlled, tethered, helium-filled balloon, an instrument/telemetry pod, a ground-based receiver/data-controller, and a ground-based support computer. Profiles of temperature, relative humidity, wind speed, and wind direction were acquired up to 1000-ft altitude before, during, and after flight testing. The weather profiler system consisted of a 10-meter tower with ten temperature sensors, five anemometers, and three wind direction sensors. The weather profiler was used to obtain detailed weather information near the ground. Weather data from both systems were acquired at a rate of at least 6 points per minute, displayed in real time, and recorded, along with time code, on magnetic disk.

Acoustic Instrumentation

A large area microphone array (Figure 4) was deployed to acquire acoustic data during this flight test program. The array consisted of 30 NASA operated, and 7 BHTI operated ground board mounted microphones arranged over a 2000-foot by almost 9000-foot area as shown in the figure. The center of the hover pad, shown as a black-filled circle, was the origin of the coordinate system used during testing (X = Y = 0). The desired flight track passed directly overhead of the line of microphones located at Y = 0, with the aircraft approaching from the -X direction towards the +X direction. The typical run terminated in an IGE hover over the hover pad. Taking advantage of the symmetry of the acoustic radiation pattern about the XV-15's longitudinal axis (Ref. 9), the microphone array was designed to measure the noise directly beneath the vehicle and off to the port side only. For the noise data presented in this paper, the representation of noise to the starboard side is the mirror image of the acoustic data measured off the port side of the vehicle. This microphone array design is useful for measuring actual ground footprints for any type of tiltrotor flight operations, and is particularly useful for quantification of the acoustic characteristics of a tiltrotor performing highly complex, non-steady state approaches. The shape of the array was designed to capture the roughly teardrop shape of the anticipated noise contours for a tiltrotor performing approaches to the hover pad. The array is widest where the noise levels were anticipated to be the greatest, and the width is reduced with increasing distance from the hover pad.

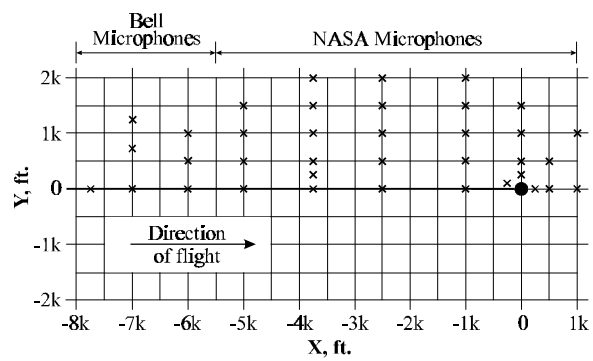

Figure 4. Microphone array configuration.

Two different types of digital data acquisition systems were used in the deployment of the 37-microphone array. The first system used NASA Langley's Digital Acoustic Recording System (DARS). With this system the microphone signals are digitized at the microphone (20 kHz sample rate), transmitted via cables to a data van, multiplexed with time and run information, and then recorded on 8-mm tape (Ref. 13). Three Langley acoustic data vans were deployed, and each data van could handle a maximum of 10 microphone systems. The second system, operated by BHTI, used a Sony PC208Ax 8-channel DAT recorder. With this system the analog microphone signals are transmitted via cables to the DAT recorder where they

are digitized (24 kHz sample rate) and recorded on 4-mm tape. The DAT recorder could handle seven microphone channels in addition to one time code channel.

On-Site Acoustic Data Processing

At the conclusion of testing each day, the 8-mm tapes containing the digitized acoustic signals from Langley's DARS were read into DEC Alpha workstations for signal processing. Likewise, the 4-mm tape containing the digitized acoustic signals from the Sony DAT recorder was read into an IBM compatible PC running the LINUX operating system. Start and stop times were selected at the endpoints in time where all data systems (acoustic, aircraft tracking and state, and weather) were simultaneously acquiring data. The digital acoustic time domain data were then transformed to the frequency domain using the average of five 4096-point FFTs with a Hamming window and 50% overlap applied, resulting in 0.6144 second blocks of data for the DARS data and 0.5120 second blocks of data for the DAT data. These averaged narrowband spectra were computed beginning every 0.5 seconds for the duration of each run. The average narrowband spectra were then integrated to obtain one-third-octave spectra, and for the DAT data only, corrections were applied to account for analog signal line losses. Line loss corrections were not required for the DARS data since the microphone signals were digitized at the microphone. The corrected one-third-octave spectra were then integrated to obtain Overall Sound Pressure Levels (OASPL). In addition, an A-weighting was applied to each one-third-octave spectrum before integration to provide A-weighted Overall Sound Pressure Levels (L_A). These L_A results were then integrated over the applicable time period for computation of Sound Exposure Level (SEL). Data plots were generally available the day following acquisition.

Flight Procedures

During this test, real-time communications were established between project control, each acoustic site, and the meteorological test site. Real-time communications were also established between project control, the XV-15 aircraft, and the TM trailer located on-site to monitor all safety-of-flight parameters. Each time the XV-15 arrived at the test site, a level flight pass was made at 60° nacelle angle and 90 knots airspeed, and a target altitude of 394 feet above ground level (AGL). These “housekeeping” passes were conducted to check the day-to-day consistency of the measurements, and as a quick check to verify the proper operation of all microphone systems.

Each approach began approximately 5 miles up-range of the microphone array, at an altitude of 1500 to 2000 feet AGL. At approximately 3 miles up-range, the desired flight procedure was initiated, and the test director radioed “prime data on.” The XV-15 continued along the flight track passing over the microphone array and decelerating to a hover at the center of the hover pad. At this point the test director radioed “prime data off” and data acquisition was discontinued. The XV-15 then climbed out and set up for the next data pass. In addition to the housekeeping pass, approximately 6 approaches were conducted during a single data flight before refueling of the aircraft was required.

Since information on handling qualities for each of the approach procedures was desired, the pilot was requested to comment on each pass. An on-board video recorder had been installed to record the flight director screen during each pass. Pilot comments were recorded on the audio track of this recorder and then transcribed for future reference.

Approach Profile Design Philosophy

Designing approach profiles that are quiet, safe, easy to fly, and repeatable requires interdisciplinary cooperation among acousticians, handling qualities experts, and pilots. Constraints are imposed by the capabilities of the specific aircraft and its control systems. For this test program, the initial candidate low-noise profiles were developed primarily using acoustic considerations, tempered with some minimal constraints concerning maximum deceleration and descent rates, along with nacelle angle conversion times. The authors used measured results from Phase 1 of the 1995 XV-15 acoustic testing (Ref. 9) as input into the Rotorcraft Noise Model (RNM) (Ref. 14). Although it was not yet complete at that time, RNM still provided a tool to assess the resulting noise produced when combining several different flight procedures into a candidate approach profile. Noise footprints produced by using different combinations of airspeed, nacelle angle, and glideslope were examined and compared with a baseline 6° glideslope, 70-knot, 85° nacelle angle approach.

A set of 10 initial candidate profiles were developed and then modified to reflect simulator experience with tiltrotor instrument approach procedures, as well as attempting to provide acceptable handling qualities. Approach profile design priorities were: First, to maximize the maneuvering portion of the approach over the 8000 feet of microphone array. Second, to aim for low noise flight conditions identified in the Phase 1 XV-15 test. Finally, the resulting profiles were adjusted

in an attempt to provide acceptable handling qualities (priority to tracking performance) for the rate-stabilized XV-15. Examples of modifications made to the approach profiles include: specifying the time required to change the glideslope (rate of flight path angle change of 0.5 degrees/second), modeling the natural braking effect produced when the nacelle angle is increased as part of selecting the deceleration rates (0.063 g deceleration matched average decelerations with nacelle moves for the XV-15), and including a 5-second buffer after a glideslope change or nacelle movement to provide time for the pilot to stabilize on the new flight condition and to prepare for the next change command. Four additional profiles were developed based on previous flight simulations done in the Vertical Motion Simulator (VMS) at NASA Ames. These procedures have acceptable handling qualities, but their noise impact was unknown.

All of the profiles discussed here were designed for "zero wind" conditions. During testing, the test site experienced significant prevailing winds that forced the XV-15 to operate with a tail wind in excess of ten knots most days, since the microphone array and the landing pad were fixed on the ground. In an attempt to accommodate these weather conditions, some of the approach profiles were modified with increased commanded (inertial) ground speed.

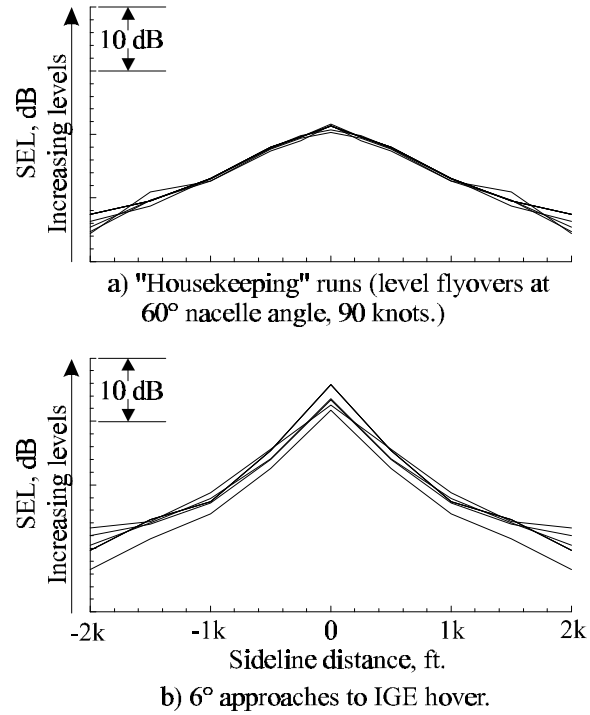

Figure 5. Sound exposure levels for multiple runs at same flight condition as measured at line of microphones 3750 feet up-range of landing point.

Results and Discussion

Data Repeatability

To examine the repeatability of the data acquired during this test program, the sound exposure levels for the most densely populated line of microphones located 3750 feet up-range are presented as a function of the sideline distance for all the housekeeping runs and for all the 6° approaches in Figures 5a and 5b, respectively. The figures show that, as one would expect, the maximum sound exposure levels were measured on the flight path centerline and the levels decrease rapidly with increasing sideline distance. For the housekeeping runs of Figure 5a, the SEL variation for the centerline microphone and all microphones up to 1000 feet to the sideline are approximately ±0.6 dB or less. The largest SEL variations are approximately ±1.6 dB for the microphones located 1500 and 2000 feet to the sideline. Figure 5b shows that the SEL variations for the 6° approaches was approximately ±2.25 dB or less for all microphones except the farthest out microphone located 2000 feet to the sideline, which had a slightly greater variation of ± 2.75 dB. These variations are consistent with what has been measured in previous XV-15 acoustic flight tests.

Approaches

Of the sixty runs flown during this test, five runs, each a different approach profile type, were selected for presentation in this paper. The first was a standard 6° approach that was derived from the 1995 XV-15 flight test program. This approach was determined to be a very comfortable (workload) approach by the pilots, with excellent handling qualities, and is also very close to a typical FAA noise certification type approach for conventional helicopters. For these reasons, the 6° approach was selected to be the "baseline" approach against which all other approach profiles would be compared. In addition to the 6° approach results, results from a 3° and a 9° approach (each with a different nacelle angle/airspeed schedule), and two 3° to 9° segmented approaches (also with different nacelle angle/airspeed schedules) are presented. The approach conditions will first be described in detail. This will be followed by a discussion of the noise footprint characteristics and a comparison against the 6° approach profile.

Approach Profiles

The primary approach profile parameters for the five selected approaches are shown in Figures 6a through 6e. Each part of the figure presents the altitude, airspeed, and nacelle angle as a function of the up-range distance for a single approach type. The initial glideslope was intercepted at a distance of 18,000 feet up-range of the landing point for all approaches. A dash-dot line indicates the intended or desired flight path. It should be noted that while the approach profiles were designed using airspeed, they were flown using ground speed. Prevailing tailwinds of approximately 10 to 15 knots persisted during most of this test, resulting in lower airspeeds than the profiles were designed for. All the profiles presented in this paper were flown in tailwinds of about 10 knots.

For the 6° approach profile (Figure 6a), the aircraft intercepted the 6° glideslope at an altitude of about 1900 feet with approximately 60 knots airspeed and a nacelle angle of 85°. This approach was designed for a 70-knot airspeed; however, 10-knot tailwinds resulted in an airspeed of about 60 knots. The 85° nacelle angle, 60 knots condition was maintained until the aircraft was approximately 3300 feet up-range, where the nacelles were rotated to 90° and a deceleration to 40 knots was begun. At about 1800 feet up-range the aircraft began decelerating to achieve an IGE hover at the landing point. As mentioned earlier, the pilot considered this to be a very comfortable approach.

For the 3° approach profile (Figure 6b), the aircraft intercepted the 3° glideslope at an altitude of about 950 feet and followed a nacelle angle/airspeed schedule very different from that of the 6° approach. This approach began with a nacelle angle of 60° and airspeed of about 100 knots. This nacelle angle and airspeed were maintained until the aircraft was 7500 feet up-range, where the nacelles were rotated to 80° and a deceleration to 60 knots was initiated. At a distance of about 3300 feet up-range, the nacelles were rotated to 85° and a deceleration to 40 knots was initiated. Finally, the nacelles were rotated to 90° at the point about 1800 feet up-range and the final deceleration to an IGE hover at the landing point was initiated. The pilot described this approach as "controllable, adequate performance and tolerable workload." However, he also commented he would have preferred to convert to a 90° nacelle angle sooner and to be allowed to convert to 95° towards the end to decrease the nose up attitude to provide a better visual view of the landing point. Conversions to 95° were not allowed due to the IFR approach constraints and for possible safety considerations in the case of an engine out.

For the 9° approach profile (Figure 6c), the aircraft intercepted the 9° glideslope at an altitude of about 2900 feet and followed the same nacelle angle/airspeed schedule as that of the 6° approach. The approach began with approximately 60 knots airspeed and a nacelle angle of 85°. At an up-range distance of about 3300 feet the nacelles were rotated to 90° and a deceleration to 40 knots was initiated. Deceleration to an IGE hover at the landing point was initiated about 1800 feet up-range. The pilot considered this to be a comfortable approach all the way in and commented "very controllable, achieved adequate performance, tolerable workload."

The 3° to 9° segmented approach profile A, shown in Figure 6d, followed a nacelle angle/airspeed schedule similar to that of the 3° approach. It had a glideslope intercept of the initial 3° glideslope at an altitude of about 1250 feet with approximately 80 knots airspeed and a nacelle angle of 60°. At a distance of about 4800 feet up-range the nacelles were rotated to 80° and a deceleration to about 60 knots was initiated. The guidance provided by the flight director system during this test did not include compensation for the aerodynamic coupling between nacelle rotation and rate of climb due to the rotation of the thrust vector. Just prior to interception of the 9° glideslope at about 2700 feet up-range and an intended altitude of about 450 feet, the aircraft deviated above the intended glideslope path by more than 100 feet due to nacelle rotation. Compensation for nacelle rotation was integrated into the flight director system during a subsequent flight director development program that is documented in Reference 11. At about 2100 feet up-range, the nacelles were rotated to 85° and a deceleration to 40 knots was begun. At about 1500 feet up-range the nacelles were rotated to 90° and the final deceleration to an IGE hover was initiated. The pilot found this approach unacceptable because "the profile keeps too high a nacelle angle for the airspeed. …don't like the (tail) buffeting vibrations on the descent."

The 3° to 9° approach profile B was designed to maintain the airspeed schedule of profile A but alter the nacelle schedule. It intercepted the initial 3° glideslope at an altitude of about 1650 feet, a nacelle angle of 80° and airspeed of 80 knots. At approximately 8700 feet up-range the nacelles we rotated to 85° and a deceleration to 70 knots was begun. The 9° glideslope was intercepted at an up-range distance of about 6200 feet and an altitude of about 1000 feet. At about 3100 feet up-range the nacelles were rotated to 90° and a deceleration to 50 knots was initiated. Finally, at about 1800 feet up-range the deceleration to an IGE hover was initiated. The increased nacelle angle schedule in this approach was an attempt to take into account the pilot's concerns from the 3° to 9° approach profile A.

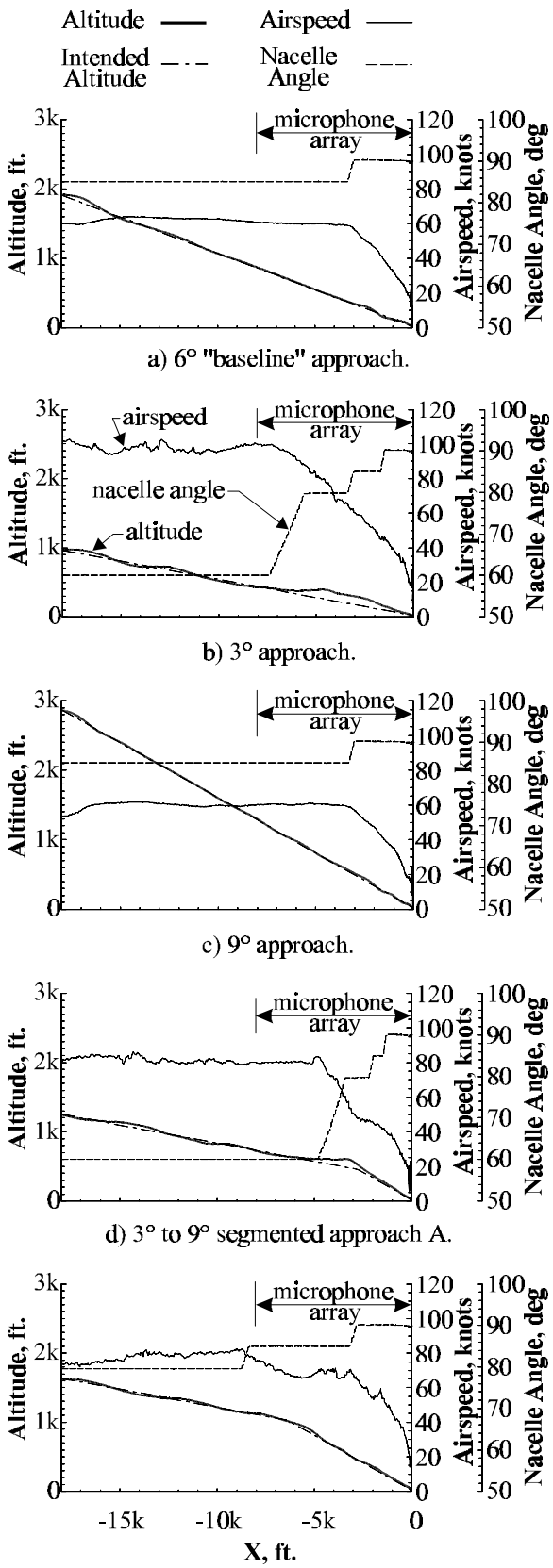

Figure 6. Approach profile characteristics.

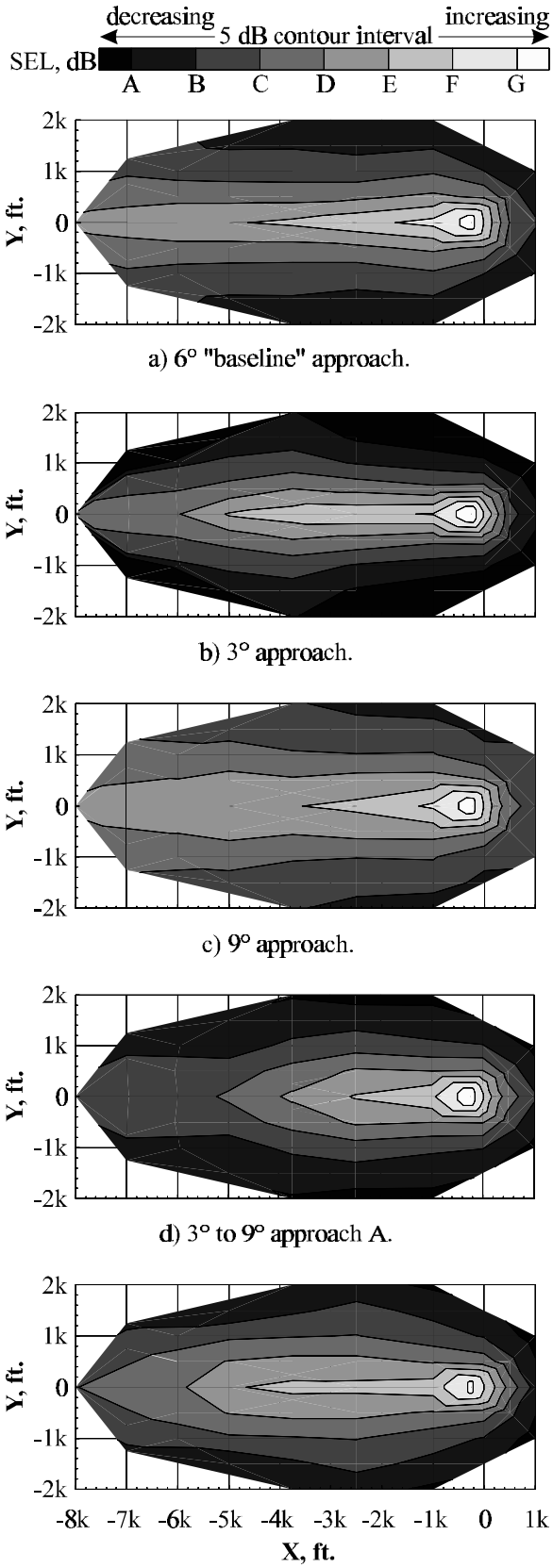

Figure 7. Sound exposure level ground contour.

The pilot indicated that this approach was much more acceptable, though there was still significant tail buffeting occurring.

Ground Contours

Figure 7 shows the characteristics of the resulting noise footprints for the same five approaches presented in Figure 6. The separation in the contour levels is 5 dBSEL and the contour levels are labeled from A to G with A representing the lowest SEL, shown as black in the figure, and G representing the highest SEL, shown as white in the figure. The contour scales for all parts of Figure 7 represent identical values to allow for direct comparisons. Each footprint extends from 1000 feet down-range to 8000 feet up-range of the landing point and spans up to 2000 feet to either side of the landing point, covering an area of more than 650 acres. The XV-15 approached from the left in the figure, along a line at Y = 0, coming to an IGE hover at about 20 feet AGL over the hover pad located at X = Y = 0. The noise footprints are most useful to provide a qualitative assessment of the noise abatement potential of the different approach profiles. The contour data will be presented in other formats later in the paper that will provide for an easier quantitative assessment.

The noise footprint for the 6° "baseline" approach is presented in Figure 7a. The highest SEL contour is located along the flight path between approximately 200 and 500 feet up-range of the hover pad ($-500 \leq X \leq -200$) and extends about 150 feet to the sidelines. The maximum SEL is not located about the hover pad due to a combination of the microphone distribution around the hover pad and the linear interpolation technique between the measurement locations used by the graphics software. Safety concerns, as well as rotor-downwash-generated wind noise, precluded locating a microphone on the hover pad. In general, the maximum levels are located about the hover point and decrease rapidly with increasing sideline distance and with increasing down-range distance. The contours decrease least rapidly along the flight path up-range of the hover point, i.e. the area the aircraft actually flies over. More specifically, the F contour level extends from about X = 0 to X = -1000 and about 250 feet to both sidelines with a narrow "tail" that extends to about 1700 feet up-range. Each successively lower SEL contour is a little larger, extending a little further in front of and to the sides of the hover pad. Up-range along the flight path the contour "tails" increase in both length and width with decreasing contour level. For the contour levels of D and below, the contour "tails" extend up-range beyond the area of the measured noise footprint.

Figure 7b shows the noise footprint for the 3° approach. Compared to the 6° approach, the contour levels generally fall off more rapidly with increasing distance from the landing point. While the E contour level extends about 500 feet further up-range, the D contour level has been shortened significantly and is contained within the boundaries of the measurement area. For the SEL contour levels below E, the decreased sideline width far up-range indicates that the up-range lengths of these contours have also been significantly decreased. This 3° approach appears to be somewhat less noisy compared to the 6° approach and in fact the average SEL for all microphones has been reduced by 3.3 dB.

The noise footprint for the 9° approach is presented in Figure 7c. Compared to the 6° approach, the contour levels generally fall off less rapidly with increasing distance from the landing point. For this approach, the E and F contour levels are a little smaller while all the contour levels below E are somewhat larger. This 9° approach appears somewhat louder than the 6° approach even though the aircraft was at a higher altitude and thus a greater distance from the microphones. The average SEL for all microphones has been increased by 1.5 dB compared to the 6° approach.

The approach footprint for the 3° to 9° approach profile A is presented in Figure 7d. All SEL contour levels for this approach are smaller when compared to those for the 6° approach. In fact, the contour levels of E and below are significantly smaller and contour levels C through G are all completely contained within the measurement area. This approach appears to be the quietest approach presented with a reduction in the average SEL of 3.6 dB.

The approach footprint for the 3° to 9° approach profile B is presented in Figure 7e. While all the SEL contour levels appear to be smaller than those for the 6° approach, they are somewhat larger than those for the 3° to 9° approach profile A. This increase is most likely due to the 80° nacelle angle during the early part of the approach compared to a 60° nacelle angle for the 3° to 9° approach A. The most significant noise reductions are at the most up-range areas for the C and D contour levels, which are both contained within the measurement area. This approach appears to be less noisy than the 6° approach but the average SEL for all microphones has been reduced by only 0.6 dB.

Sideline Sound Exposure Levels

To provide a more quantitative assessment of the SEL differences for the different approach profiles,

Figure 8 presents the SELs as a function of the sideline distance for a number of slices across the noise footprint. More specifically, Figures 8a through 8f present the SELs for the five approaches as a function of sideline distance for slices across the noise footprint located 1000, 2500, 3750, 5000, 6000, and 7000 feet up-range of the landing point, respectively.

For the slice 1000 feet up-range, Figure 8a shows that the maximum levels were measured on the centerline and the levels fall off quickly with increasing sideline distance. On the centerline, the 6° approach has the highest SEL while the 3° to 9° approach B has the lowest SEL and the difference is about 4 dB. However, for the sideline measurement locations the 9° approach generally has the highest SEL while the 3° to 9° approach A has by far the lowest SEL. At the 1500-foot sideline distance the 3° to 9° approach A is almost 10 dBSEL lower than the 9° approach and more than 7 dB lower than the 6° approach.

Moving further up-range to the 2500 foot slice shown in Figure 8b, the 3° and 6° approaches have the highest levels on the centerline while all the other approaches are about 3 dB lower. For all sideline measurement locations the 3° approach has the lowest level. At 2000 feet to the sideline the 3° approach is almost 6 dB lower than the 6° approach.

At 3750 feet up-range the 3° and 6° approaches again have the highest levels on centerline, along with the 3° to 9° approach B. The 3° to 9° approach A had the lowest levels on centerline and at all the sideline measurement locations. Compared to the 6° approach, this approach is about 6dB down on centerline and about 3 dB down at 2000 feet to the sideline. The 9°

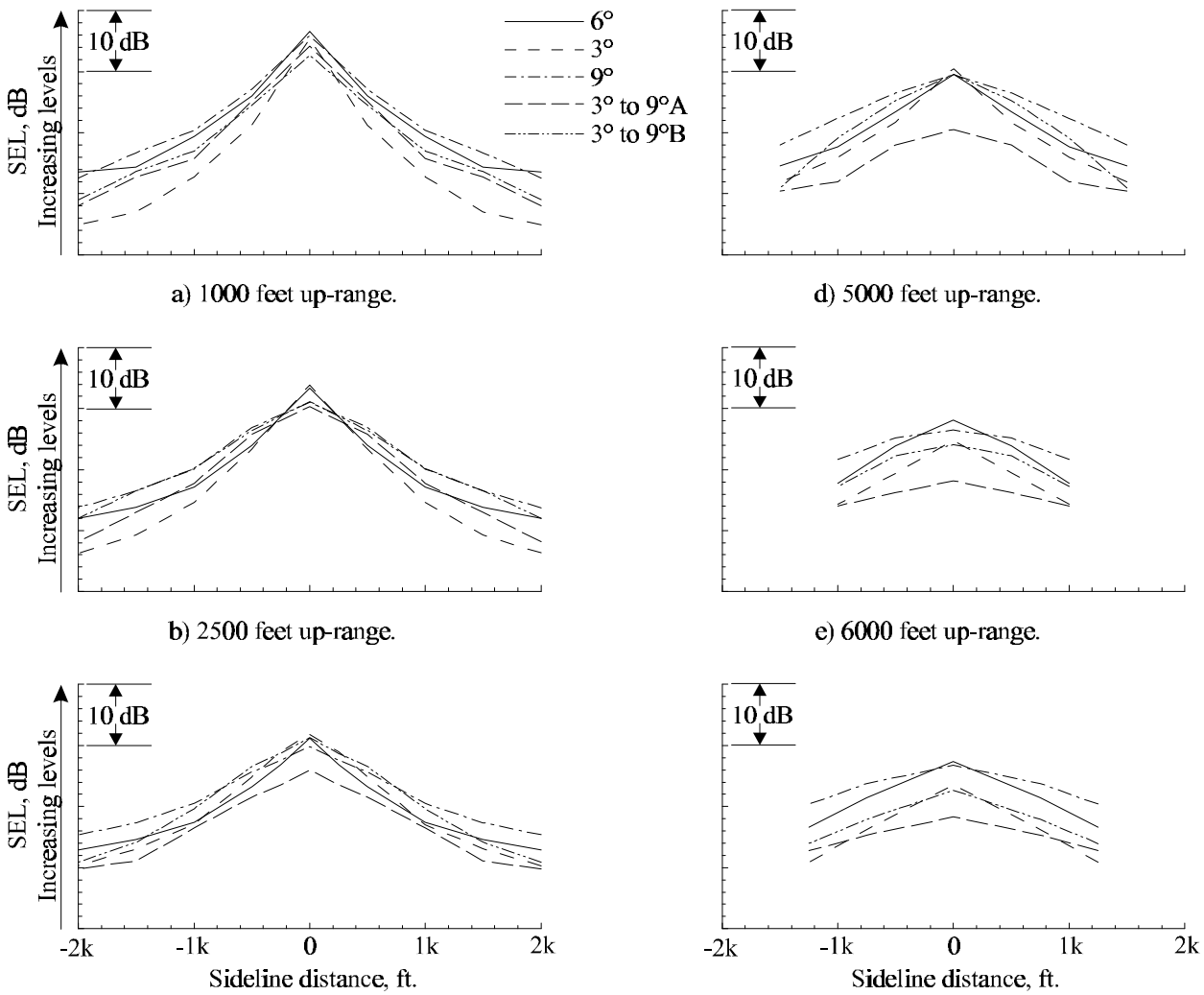

a) 1000 feet up-range.

b) 2500 feet up-range.

c) 3750 feet up-range.

d) 5000 feet up-range.

e) 6000 feet up-range.

f) 7000 feet up-range.

Figure 8. Sound exposure levels as a function of sideline distance.

the three outermost sideline locations and are about 2 to 3 dB higher than the 6° approach.

At 5000 feet up-range (Figure 8d) all approaches have about the same centerline SEL with the exception of the 3° to 9° approach A, which is almost 10 dB down. Again, the 3° to 9° approach A has the lowest levels for all measurement locations and is about 4 to 6 dB down from the 6° approach at all sideline locations. At between 3 and 5 dB higher than the 6° approach, the 9° approach has the highest levels on the sidelines.

At 6000 feet up-range, the 6° approach has the highest level on centerline while the 9° approach has the highest levels at all sideline locations. Once again, the 3° to 9° approach A has the lowest levels at all measurement locations. Compared to the 6° approach, this approach is 10 dB down on centerline and between 4 and 6 dB down on the sidelines.

The 6° approach is again the highest on centerline at 7000 feet up-range (Figure 8f) and the 9° approach is highest on the sidelines. The 3° to 9° approach A is lowest on centerline and at 750 feet to the sideline; however, the 3° approach is lowest 1250 feet to the sideline. Compared to the 6° approach, the 3° to 9° approach A is about 9 dB down on centerline and about 6 dB down at the sideline locations.

As a function of up-range distance, Figure 8 shows that the SEL variation on centerline for the five approaches increased from a minimum of about 4 dB 1000 feet up-range to a maximum of nearly 10 dB at 5000 feet and further up-range. The 6° approach had the highest levels, or very nearly the highest levels, on centerline at all up-range distances. The 9° approach tended to have the highest levels for all the sideline measurement locations at all the up-range distances. The 3° approach had some of the highest levels on centerline for up-range distances up to 5000 feet while simultaneously having some of the lowest levels at the sideline measurement locations. At up-range distances of 6000 and 7000 feet, the 3° approach had some of the lowest sideline levels and moderate centerline levels. While being pretty much middle of the pack at 1000 and 2500 feet up-range, the 3° to 9° approach A had the lowest levels for nearly all measurement locations from 3750 feet to 7000 feet up-range, in many cases by a large margin. This approach has lower noise levels earlier in the approach during the quieter 3° approach segment and higher levels near the end of the approach during the louder 9° approach segment. The 3° to 9° approach B did not seem to benefit from the 3° approach segment, probably because of the higher 80° nacelle angle compared to a 60° nacelle angle during much of the 3° approach, and during the 3° portion of the 3° to 9° approach A.

Average Sound Exposure Levels

Another type of assessment of the SEL differences for the different approach profiles that is more quantitative is to compare the average SEL (AVGSEL) for all microphones, or for a given subset of the microphones. Figure 9a and Table 1 identify the different microphone sets which were averaged and presented here. Figure 9b presents the difference between the average SEL for the 6° approach and the average SEL for each of the other approaches as a function of the microphone set. A negative ΔAVGSEL means that the average SEL has been reduced compared to the 6° baseline approach. This figure shows that the 9° approach had the highest levels for all microphone sets presented with a ΔAVGSEL of between 1 and 2 dB. The 3° to 9° approach profile B was about 1 dBSEL quieter than the baseline for all microphone sets except Set D which was a little more than 3 dBSEL quieter. The 3° approach is the quietest approach around the landing point (Set A) with a ΔAVGSEL of about –5.5 dB. This may be because the lower rate of descent requires less of a flare at the end of the approach to achieve a hover condition. For the average SEL using all the microphones (Set B), the 3° approach is a little more than 3 dBSEL quieter than the baseline approach while Sets C and D show less noise reduction with ΔAVGSELs of about –1.5 and –3 dBSEL, respectively. The 3° to 9° approach profile A shows the greatest noise reduction for all microphone sets except around the hover pad. The noise benefits for this approach increase as you move to the progressively up-range microphone sets. For Set D, the average SEL has been reduced by more than 7 dBSEL compared to the 6° baseline approach.

Table 1. Microphone set ID.

Microphone set ID	Microphones used in average
A	All microphones between 1000 feet down-range and 1000 feet up-range of the landing point
B	All microphones
C	All microphones between 3000 and 8000 feet up-range of the landing point
D	All microphones between 6000 and 8000 feet up-range of the landing point

This figure indicates that the 3° to 9° approach profile A provides the greatest noise abatement for all areas of the measured footprint except near the landing point.

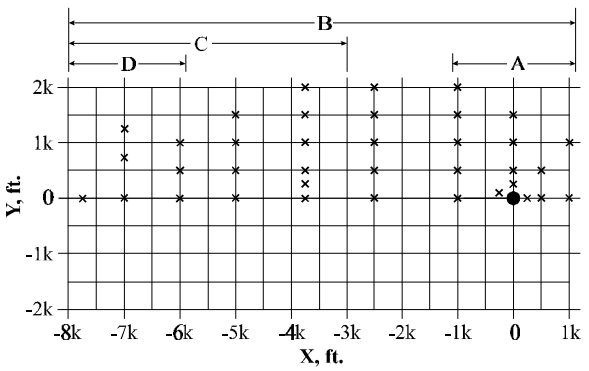

a) Microphone set ID

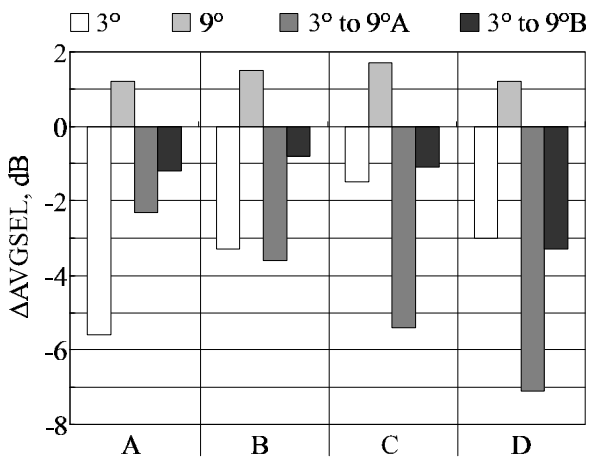

b) SEL difference from 6° baseline approach.

Figure 9. Average SEL difference for different microphone sets.

Contour Areas

One more way to assess the noise abatement potential of the different approach profiles is to compare the ground contour areas exposed to a given noise level. Figure 10 presents the contour area in percentage of the total measurement area as a function of the relative SEL for the five different approaches. At the lowest levels, all the approaches converge to 100% of the measurement area. At the highest levels, all approaches eventually converge to 0% of the measurement area. For a given contour area, the largest differences in areas between the different approaches are found at the lowest noise levels while the smallest differences are found at the highest noise levels. This figure clearly shows that the 9° approach had the largest contour areas for all but the highest levels. The curves for the 6° approach and the 3° to 9° approach B are very similar except at the lower levels, where the contour area for the 6° approach is larger. The 3° approach and the 3° to 9° approach A have the smallest contour areas for all levels except the very highest, where the areas are quite small anyway. The 3° approach has smaller areas at the lower levels while the 3° to 9° approach A has smaller areas at the moderate levels. This figure also clearly demonstrates that the 3° approach and the 3° to 9° approach A are the quietest runs considered in this paper.

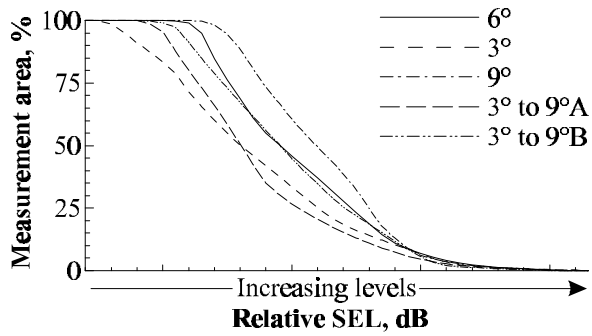

Figure 10. Sound exposure level ground contour areas as a percentage of total measurement area.

Impact of the Flight Director and Handling Qualities on Noise Abatement Procedures

In previous testing (Ref. 9), no formal flight director was available, and the target profiles were flown as "Visual Flight Rules" (VFR) approaches. Although a localizer-type needle was available to give lateral position indications, the pilot used predominantly "heads-up" visual cues for each approach. This allowed the transition from airplane mode to begin relatively near the touchdown point. In these earlier tests, the noise reduction flexibility of the tiltrotor was clearly apparent, since the aircraft remained in the relatively quiet low-nacelle flight regime until very near the landing point. In some cases, the full transition from airplane mode to helicopter mode was performed over the microphone array.

In the present test, the profiles were flown as "Instrument Flight Rules" (IFR) approaches using the newly developed flight director. This allowed much more repeatable, precise profiles, but ones which were necessarily limited by the pilot's IFR workload. To allow enough time for the pilot to assimilate the flight director's visual cues and translate them into control inputs, an approximately 5 second time delay, or buffer, had to be allowed for after each pilot instruction. This buffer produced an elongated approach.

The attempt to concentrate active approach maneuvering over the microphone array resulted in approach profile planning segments more aggressive than suggested for routine instrument operations, as derived from simulator experience (Ref. 12). Experience with simulated tiltrotor instrument approaches suggests keeping the aircraft pitch attitude modest and making gentle flight condition changes. Evidence of pilot workload increase came from both handling qualities commentary and task performance and also was indicated by tracking performance. Figure 11 exemplifies the results of high pilot workload. This profile featured a two-segment 3° to 6° approach. Profile airspeed commands attempted to continuously decelerate on the two-segment approach path, with no "settling time" breaks. As shown in Figure 11a, the aircraft decelerated too rapidly prior to the glide slope break between the 3° and 6° flight path angles at X = -4500 feet. The rapid deceleration combined with the nacelle change from 60° to 80° resulted in the aircraft initially rising over and then rapidly dropping under the intended flight path. Pilot commentary pointed to the difficulty faced by the pilot with so many rapid changes in flight condition. The resulting noise footprint, seen in Figure 11b, shows a noise "hot spot" as a result of poor altitude and airspeed tracking. Subsequent flight profiles provided the five second buffer between major flight condition changes. Modest flight condition changes, such as 5° nacelle movements, gentle commanded decelerations and appropriate buffer times resulted in much tighter tracking of the intended flight profile.

The data from this test indicate the XV-15 was at much higher nacelle angles (60° to 85°) while over the microphone array than was the case in previous testing. This was, of course, a natural result of the progression to the new flight director, but it limited the terminal area noise-reduction potential. Improvements in control systems and future flight directors will allow the quieter low-nacelle flight operations to be brought nearer the terminal area. As higher levels of control augmentation and other improvements are incorporated, future pilot workload will be reduced, allowing precise, repeatable approaches to be made in a shorter time/distance interval. This will allow approaches that *tend* more toward the shorter VFR-type approaches.

Within the next 10 years, civil tiltrotor operations will make use of the information derived from both VFR- and IFR-type acoustic testing to combine handling qualities and acoustic constraints in a highly efficient flight director. This will allow the noise-reduction potential of the tiltrotor to be applied in precise, repeatable approaches to the public benefit.

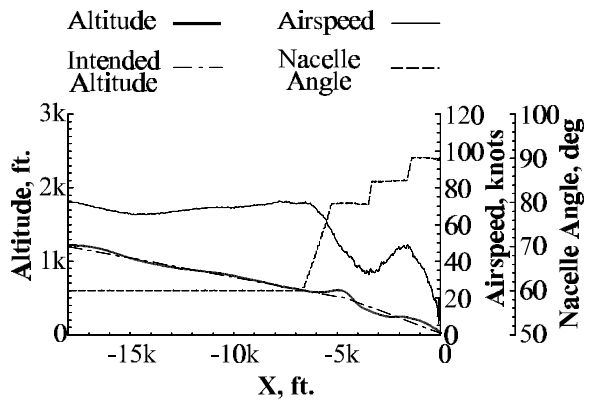

a) Approach profile characteristics.

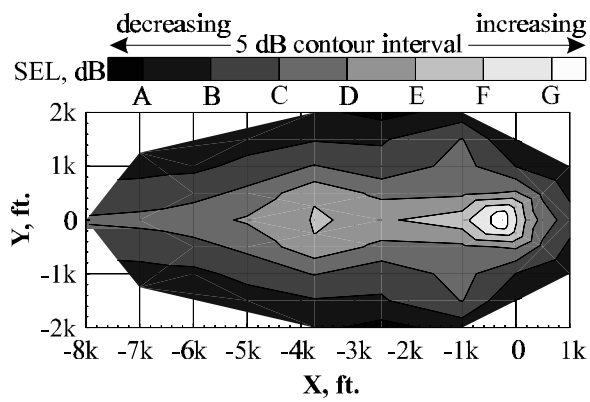

b) Sound exposure level ground contour.

Figure 11. Example of approach with high pilot workload.

Summary of Noise Abatement Approaches

All of the above results lead the authors to make the following assessments. The 3° approach and the 3° to 9° segmented approach profile A were the quietest approaches tested during this program. This is primarily due to the fact that these approaches maintained a lower 60° nacelle angle until about one-mile from the landing point. The combination of nacelle angle, airspeed, and glideslope appear to orient the rotors tip-path-planes to a condition that avoids blade-vortex interactions (BVI). All the other approaches presented here began at a nacelle angle of 80° from nearly three miles out, thus putting the rotors into a flight condition more likely to generate BVI noise. The 3° approach was the quietest around the hover pad, probably due to the lower descent rate requiring less of a decelerating flare to achieve hover at the landing point. The 3° to 9° segmented approach profile A was much quieter at the far up-range distances, probably because the aircraft was on the

quieter 3° glideslope but about 300 feet higher in altitude than the 3° approach due to the steeper 9° segment towards the end of the approach. For the final portion of the approach, from about 2500 feet up-range to the landing point, the 3° to 9° segmented approach profile A was quieter on and around the centerline of the flight path while the 3° approach was quieter to the sidelines. This was probably because the 3° to 9° approach had transitioned to the noisier condition of the 9° glideslope. Comparing the 3°, 6°, and 9° approaches, the 6° approach tended to be the loudest on centerline at all up-range distances measured; however, this difference was usually quite small. The noise levels to the sidelines at all up-range distances increased with increasing glideslope angle. Noise levels around the landing point also increased with increasing glideslope angle. Overall, the 9° approach was the loudest and the 3° approach was the quietest. The 3° to 9° segmented approach profile B was quieter than the 6° and 9° approaches, but not by much except at the far up-range distances. This approach was much noisier than the 3° to 9° segmented approach profile A, probably because the higher 80° nacelle angle employed during the early portion of the approach put the rotor into a condition where BVI noise was generated.

Concluding Remarks

Acoustic measurements were obtained for the XV-15 tiltrotor aircraft performing a large number of different approach profiles. Approaches were flown over a large area microphone array to measure the noise footprint of the XV-15 during different flight approach profiles. Five different approach profiles are presented in this paper – 3°, 6°, and 9° approaches and two different 3° to 9° segmented approaches. The 6° approach was considered the "baseline" approach and all other approaches are compared against it. Handling qualities considerations played an important role in the design of the noise abatement approach profiles. A newly developed flight director allowed much more repeatable and precise profiles to be flown but simultaneously limited the noise abatement potential due to the high pilot workload required to fly these IFR type approaches. The data set was found to have good repeatability for matching flight conditions with a variation of ±0.6 dBSEL on centerline for level flyovers and ±2.25 dBSEL variation on centerline, 3750 feet back from the landing point for 6° approaches. The 9° approach was found to be the loudest approach with an average SEL about 1.5 dB higher than that for the 6° baseline approach. The 6° approach had the highest centerline levels at all up-range distances while the 9° approach tended to have the highest sideline levels. The 3° approach was found to be one of the quieter profiles overall with an average SEL about 3.25 dB down from the baseline approach. However, most of the noise reduction was found to the sidelines with very little, if any, noise reduction on the centerline except at the farthest up-range measurement locations. One of the 3° to 9° segmented approaches was found to be the quietest approach with an average 3.6 dBSEL reduction compared to the baseline approach. This approach provided the greatest noise abatement benefits at the farther up-range locations during the 3° approach angle segment and less benefits close to the landing point during the 9° segment. Noise reductions of as much as 10 dBSEL were found at the up-range centerline locations about one mile out and beyond. The average SEL reduction for all microphones from 4000 to 8000 feet up-range was almost 7 dB.

The noise reductions measured reflect lower BVI noise generation that results from more favorable nacelle angle/airspeed/glideslope schedules. The data strongly suggests approaching at nacelle angles no higher than about 60°, and maintaining these low nacelle angles for as long as possible. This has been demonstrated in the quieter 3° approach and the 3° to 9° segmented approach profile A cases, where there is a clear reduction in source noise due directly to the scheduling of primarily the nacelle angle. Nacelle angle is a configuration control (and primary acceleration control at low speed) unique to the tiltrotor that can be used to achieve noise abatement. The results also clearly indicate that nacelle angle/airspeed/glideslope schedules can be developed to achieve maximum noise abatement for all profiles envisioned for IFR type approaches.

Repeatability of optimum noise abatement approach profiles can be assured with use of a flight director. Further improvements in the tiltrotor's flight director and simulation studies will allow this optimization to take place in all segments of the approach and landing.

Acknowledgments

The authors would like to recognize the efforts of all of the personnel involved with the test program from Bell Helicopter Textron, Inc., NASA Ames and Langley Research Centers, the U. S. Army, and the associated contractors affiliated with these organizations. Without the extreme dedication of all of the people involved with the test program, the test would not have been a success. However, a few individuals and groups deserve special recognition for their efforts. These included Bell personnel Bill Martin for his work with the XV-15, Mark Stoufflet for his work developing and supporting the excellent real-time field displays of the tracking data, and Kelly Spivey for quickly processing all the XV-15

on-board data. The field measurement team from Wyle Labs deserve special accolades for always having the acoustic measurement systems ready for testing and for keeping the weather balloon aloft on demand. Obviously, this test could not have been successful without the diligent efforts of the pilots, Roy Hopkins, John Ball, and Ron Erhart of Bell and Rick Simmons of NASA Ames. Finally, Charles Smith of Lockheed Martin Engineering and Sciences Co., deserves an enormous amount of credit for processing all of the acoustic data acquired during this test program while on-site, as well as assimilating all of the different types of data into one comprehensive data set. This paper would have been impossible without his efforts.

References

1. Huston, R.J., Golub, R.A., and Yu, J.C., "Noise Considerations for Tiltrotor," AIAA Paper No. 89-2359, 1989.

2. George, A.R., Smith, C.A., Maisel, M.D., and Brieger, J.T., "Tilt Rotor Aircraft Aeroacoustics," Presented at the American Helicopter Society 45th Annual Forum, Boston, MA, May 22-24, 1989.

3. Lee, A., and Mosher, M., "An Acoustical Study of the XV-15 Tilt Rotor Research Aircraft," AIAA Paper No. 79-0612, 1979.

4. Maisel, M., and Harris, D., "Hover Tests of the XV-15 Tilt Rotor Research Aircraft," AIAA Paper No. 81-2501, 1981.

5. Conner, D.A., and Wellman, J.B., "Hover Acoustic Characteristics of the XV-15 with Advanced Technology Blades," AIAA Journal of Aircraft, Volume 31, Number 4, July-August 1994.

6. Brieger, J.T., Maisel, M.D., and Gerdes, R., "External Noise Evaluation of the XV-15 Tilt Rotor Aircraft," Presented at the AHS National Technical Specialists' Meeting on Aerodynamics and Aeroacoustics, Arlington, TX, February 25-27, 1987.

7. Edwards, B.D., "XV-15 Tiltrotor Aircraft Noise Characteristics," Presented at the American Helicopter Society 46th Annual Forum, Washington, DC, May 21-23, 1990.

8. Marcolini, M.A., Conner, D.A., Brieger, J.T., Becker, L.E., and Smith, C.D., "Noise Characteristics of a Model Tiltrotor," Presented at the American Helicopter Society Forum 51, Fort Worth, TX, May 9-11, 1995.

9. Conner, D.A., Marcolini, M.A., Edwards, B.D., and Brieger, J.T., "XV-15 Tiltrotor Low Noise Terminal Area Operations," Presented at the American Helicopter Society 53rd Annual Forum, Virginia Beach, VA, April 29 - May 1, 1997.

10. "Tilt Rotor Research Aircraft Familiarization Document," NASA TMX-62,407, Jan. 1975.

11. Klein, P.D., and Nicks, C.O., "Flight Director and Approach Profile Development for Civil Tiltrotor Terminal Area Operations," Presented at the American Helicopter Society 54th Annual Forum, Washington, DC, May 1998.

12. Decker, W. A, "Piloted Simulator Investigations of a Civil Tilt-Rotor Aircraft on Steep Instrument Approaches," AHS 48th Annual Forum, Washington, DC, June 1992.

13. Gray, D., Wright, K., and Rowland, W., "A Field-Deployable Digital Acoustic Measurement System," Presented at Technology 2000 (Proceedings published as NASA CP 3109, Vol. 2), Washington, DC, November 27-28, 1990.

14. Lucas, M.J., and Marcolini, M.A., "Rotorcraft Noise Model," Presented at the AHS Technical Specialists' Meeting for Rotorcraft Acoustics and Aerodynamics, Williamsburg, VA, October 28-30, 1997.